

ENO Reconstruction and ENO Interpolation Are Stable

Ulrik S. Fjordholm, Siddhartha Mishra & Eitan Tadmor

Foundations of Computational Mathematics

The Journal of the Society for the Foundations of Computational Mathematics

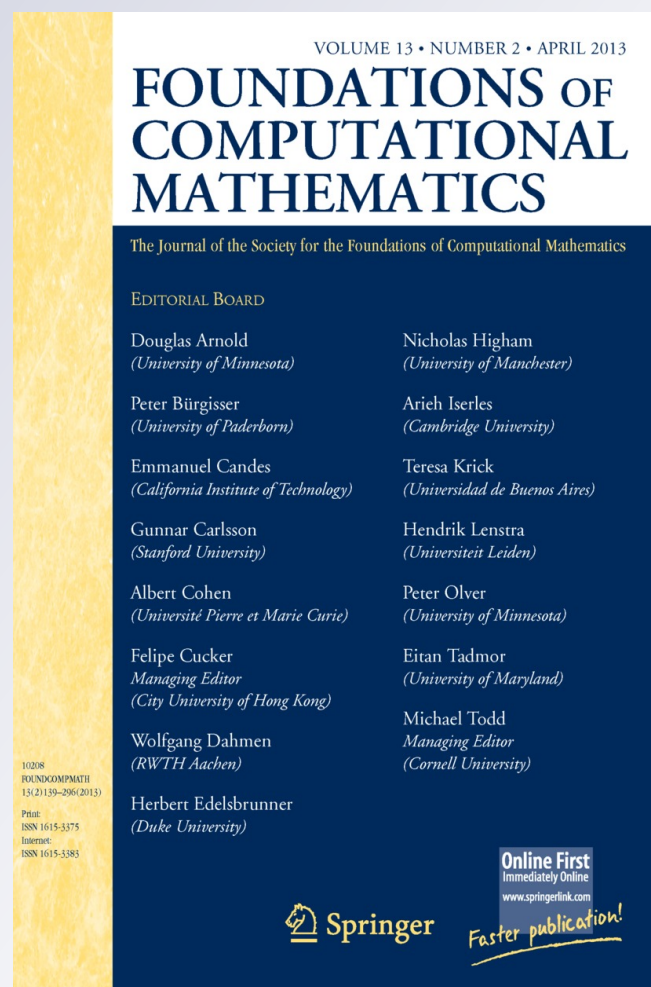
ISSN 1615-3375

Volume 13

Number 2

Found Comput Math (2013) 13:139-159

DOI 10.1007/s10208-012-9117-9



Your article is protected by copyright and all rights are held exclusively by SFoCM. This e-offprint is for personal use only and shall not be self-archived in electronic repositories. If you wish to self-archive your work, please use the accepted author's version for posting to your own website or your institution's repository. You may further deposit the accepted author's version on a funder's repository at a funder's request, provided it is not made publicly available until 12 months after publication.

ENO Reconstruction and ENO Interpolation Are Stable

Ulrik S. Fjordholm · Siddhartha Mishra ·
Eitan Tadmor

Received: 5 May 2011 / Revised: 26 November 2011 / Accepted: 16 January 2012 /
Published online: 28 March 2012
© SFoCM 2012

Abstract We prove that the ENO reconstruction and ENO interpolation procedures are stable in the sense that the jump of the reconstructed ENO point values at each cell interface has the same sign as the jump of the underlying cell averages across that interface. Moreover, we prove that the size of these jumps after reconstruction relative to the jump of the underlying cell averages is bounded. Similar sign properties and the boundedness of the jumps hold for the ENO interpolation procedure. These estimates, which are shown to hold for ENO reconstruction and interpolation of arbitrary order of accuracy and on nonuniform meshes, indicate a remarkable rigidity of the piecewise polynomial ENO procedure.

Keywords Newton interpolation · Adaptivity · ENO reconstruction · Sign property

Mathematics Subject Classification 65D05 · 65M12

Communicated by Nira Dyn.

U.S. Fjordholm · S. Mishra
Seminar for Applied Mathematics, ETH Zürich, HG J 48, Rämistrasse 101, Zürich, Switzerland

U.S. Fjordholm
e-mail: ulrikf@sam.math.ethz.ch

S. Mishra
e-mail: semishra@sam.math.ethz.ch

E. Tadmor (✉)
Department of Mathematics, Center of Scientific Computation and Mathematical Modeling (CSCAMM), Institute for Physical Sciences and Technology (IPST), University of Maryland, College Park, MD 20742-4015, USA
e-mail: tadmor@cscamm.umd.edu

1 Introduction and Statement of Main Results

The acronym ENO in the title of this paper stands for “essentially non-oscillatory,” and it refers to a *reconstruction* procedure that generates a piecewise polynomial approximation of a function from a given set of its cell averages. The essence of the ENO procedure, which was introduced by Harten et al. [16], is its ability to accurately recover discontinuous functions. The starting point is a collection of cell averages $\{\bar{v}_i\}_{i \in \mathbb{Z}}$ over consecutive intervals $I_i = [x_{i-1/2}, x_{i+1/2})$,

$$\bar{v}_i := \frac{1}{|I_i|} \int_{I_i} v(x) \, dx, \tag{1.1}$$

from which one can form the piecewise constant approximation of the underlying function $v(x)$,

$$\mathcal{A}v(x) := \sum_k \bar{v}_k \mathbb{1}_{I_k}(x), \quad \mathbb{1}_{I_k}(x) = \begin{cases} 1 & \text{if } x \in I_k, \\ 0 & \text{if } x \notin I_k. \end{cases}$$

But the averaging operator $\mathcal{A}v(x)$ is limited to first-order accuracy, whether v is smooth or not; for example, if v has bounded variation, then $\|v - \mathcal{A}v\|_{L^1} = \mathcal{O}(h)$ where $h := \max_i |I_i|$. The purpose of the ENO procedure (abbreviated as \mathcal{R}) is to reconstruct a higher order approximation of $v(x)$ from its given cell averages,

$$\text{ENO: } \mathcal{A}v(x) = \sum_k \bar{v}_k \mathbb{1}_{I_k}(x) \mapsto \mathcal{R}\mathcal{A}v(x) := \sum_k f_k(x) \mathbb{1}_{I_k}(x). \tag{1.2}$$

Here, $f_k(x)$ are polynomials of degree $p - 1$ such that the piecewise polynomial ENO reconstruction $\mathcal{R}\mathcal{A}v(x)$ satisfies the following two essential properties:

Accuracy: First, it is an approximation of $v(x)$ of order p in the sense that

$$\mathcal{R}\mathcal{A}v(x) = v(x) + \mathcal{O}(h^p), \quad h = \max_i |I_i|. \tag{1.3}$$

Typically, the requirement for accuracy is sought whenever $v(\cdot)$ is sufficiently smooth in a neighborhood of x . But here, (1.3) is also sought at isolated points of jump discontinuities. Thus, if we let $v(x_{i+1/2+})$ and $v(x_{i+1/2-})$ denote the point values of $v(x)$ at the left and right of the interface at $x_{i+1/2}$, then (1.3) requires that the corresponding reconstructed point values, $v_{i+1/2}^- := \mathcal{R}\mathcal{A}v(x_{i+1/2-}) = f_i(x_{i+1/2})$ and $v_{i+1/2}^+ := \mathcal{R}\mathcal{A}v(x_{i+1/2+}) = f_{i+1}(x_{i+1/2})$, satisfy

$$|v_{i+1/2}^- - v(x_{i+1/2-})| + |v_{i+1/2}^+ - v(x_{i+1/2+})| = \mathcal{O}(h^p).$$

To address this requirement of accuracy, the f_i 's are constructed from neighboring cell averages $\{\bar{v}_{i+j}\}_{j=k}^{k+p-1}$ for some $k \in \{-p + 1, \dots, 0\}$. The key point is to choose an *adaptive stencil*,

$$i \mapsto \{\bar{v}_{i+k}, \dots, \bar{v}_i, \dots, \bar{v}_{i+k+p-1}\},$$

based on a data-dependent shift $k = k(i)$. This enables the essential non-oscillatory property (1.3), while making the ENO procedure *essentially nonlinear*.

Conservation: The second property sought in the ENO reconstruction is that the piecewise polynomial ENO approximation be *conservative*, in the sense of conserving the original cell averages,

$$\frac{1}{|I_i|} \int_{I_i} \mathcal{R}\mathcal{A} v(x) \, dx = \bar{v}_i. \tag{1.4}$$

The conservative property enables us to recast the ENO procedure in an equivalent formulation of nonlinear *interpolation*. To this end, let $V(x) := \int_{-\infty}^x v(s) \, ds$ denote the primitive of $v(x)$. The given cell averages $\{\bar{v}_i\}$ now produce a set of point values $\{V_{j+1/2}\}_{j \in \mathbb{Z}}$,

$$V_{j+1/2} := \int_{-\infty}^{x_{j+1/2}} v(s) \, ds = \sum_{k=-\infty}^j \int_{x_{k-1/2}}^{x_{k+1/2}} v(s) \, ds = \sum_{k=-\infty}^j |I_k| \bar{v}_k. \tag{1.5}$$

A second-order approximation of these point values is given by the piecewise linear interpolant $\mathcal{L}V(x) := \sum_k \frac{1}{|I_k|} (V_{k-1/2}(x_{k+1/2} - x) + V_{k+1/2}(x - x_{k-1/2})) \mathbb{1}_{I_k}(x)$. The ENO approximation, $\sum_k F_k(x) \mathbb{1}_{I_k}(x)$, is a higher order accurate piecewise polynomial interpolant,

$$\text{ENO: } \mathcal{L}V(x) \mapsto \mathcal{R}\mathcal{L}V(x) := \sum_k F_k(x) \mathbb{1}_{I_k}(x). \tag{1.6}$$

It interpolates the given data at the nodes, $F_i(x_{i \pm 1/2}) = V_{i \pm 1/2}$, and it recovers $V(x)$ to high-order accuracy at the interior of the cells, $\mathcal{R}\mathcal{L}V(x) = V(x) + \mathcal{O}(h^{p+1})$. Now, let $F_i(x)$ be the unique p th order polynomial interpolating the $p + 1$ point values $V_{i+r}, \dots, V_{i+r+p}$ for some shift r which is yet to be determined. Then, as a simple consequence of (1.5), f satisfies (1.3) and (1.4) and

$$F_i(x) = V_{i-1/2} + \int_{x_{i-1/2}}^x f_i(s) \, ds.$$

In this manner, ENO reconstruction of cell averages is equivalent to ENO interpolation of the point values of its primitive. We shall travel back and forth between these two ENO formulations.

Note that there are other approaches for ENO reconstruction of point values, $\{v_{i+1/2}^\pm\}$, from cell averages, $\{\bar{v}_{i+k}\}$, such that the above properties of accuracy and conservation hold, e.g., reconstruction via deconvolution [16].

1.1 ENO Reconstruction

When the underlying data are sufficiently smooth, the accuracy requirements can be met by interpolating the primitive V on *any* set of $p + 1$ point values

$$\{V_{i+r}, \dots, V_{i-1/2}, V_{i+1/2}, \dots, V_{i+r+p}\}.$$

Here, r is the (left) *offset* of the interpolation stencil, which is indexed at *half-integers*, to match the cell interfaces. To satisfy the conservation property (1.4), the stencil of interpolation must include $V_{i-1/2}$ and $V_{i+1/2}$. There are p such stencils, ranging from the leftmost stencil corresponding to an offset $r = -p + 1/2$ to the rightmost stencil corresponding to an offset of $r = -1/2$. Since we are interested in approximation of piecewise smooth functions, we must choose a carefully shifted stencil, in order to avoid spurious oscillations. The main idea behind the ENO procedure is the use of a stencil with a data-dependent offset, $r = r(i)$, which is *adapted to the smoothness of the data*. The choice of ENO stencil is accomplished in an iterative manner, based on divided differences of the data.

Algorithm 1.1 (ENO Reconstruction Algorithm: Selection of ENO Stencil) Let point values of the primitive $V_{i-p+1/2}, \dots, V_{i+p-1/2}$ be given, e.g., (1.5):

- Set $r_1 = -1/2$.
- For each $j = 1, \dots, p - 1$, do:

$$\left\{ \begin{array}{l} \text{if } |V[x_{i+r_j-1}, \dots, x_{i+r_j+j}]| < |V[x_{i+r_j}, \dots, x_{i+r_j+j+1}]| \\ \quad \mapsto \text{ set } r_{j+1} = r_j - 1, \\ \text{otherwise } \mapsto \text{ set } r_{j+1} = r_j. \end{array} \right.$$

- Set $F_i(x)$ as the interpolant of V over the stencil $\{V_{i+k}\}_{k=r_p}^{r_p+p}$.
- Compute $f_i(x) := F'_i(x)$.

The divided differences $V[x_k, \dots, x_{k+j}]$ are a good measure of the j th order of smoothness of $V(x)$. Thus, the ENO procedure is based on data-dependent stencils which are chosen in the *direction of smoothness*, in the sense of preferring the smallest divided differences.

The ENO reconstruction procedure was introduced in 1987 by Harten et al. [15, 16] in the context of accurate simulations for piecewise smooth solutions of nonlinear conservation laws. Since then, the ENO procedure and its extensions [10–13, 21, 23] have been used with considerable success in computational fluid dynamics; we refer to the review article of Shu [22] and the references therein. Moreover, ENO and its various extensions, in particular, ENO schemes with subcell resolution (ENO-SR) [10], have been applied to problems in data compression and image processing in [1–4, 6, 7, 14, 19] and references therein.

There are only a few rigorous results about the global accuracy of the ENO procedure. In [2], the authors proved the second-order accuracy of ENO-SR reconstruction of piecewise smooth C^2 data. Multidimensional global accuracy results for the ENO-EA method were obtained in [3]. A modified ENO reconstruction which yields positivity preserving (on a uniform mesh) at the expense of sacrificing high accuracy was derived in [5]. Despite the extensive literature on the construction and implementation of the ENO method and its variants for the last 25 years, we are not aware of any global, mesh-independent, *stability* properties. This brings us to the main result of this paper, stating the stability of the ENO reconstruction procedure in terms of the following sign property.

Theorem 1.1 (The Sign Property) *Fix an integer $p > 1$. Given the cell averages $\{\bar{v}_i\}$, let $\mathcal{R}\mathcal{A}v(x)$ be the p th order ENO reconstruction of these averages, as outlined in Algorithm 1.1,*

$$\mathcal{R}\mathcal{A}v(x) = \sum_k f_k(x)\mathbb{1}_{I_k}(x), \quad \deg f_k(x) \leq p - 1.$$

Let $v_{i+1/2}^+ := \mathcal{R}\mathcal{A}v(x_{i+1/2+})$ and $v_{i+1/2}^- := \mathcal{R}\mathcal{A}v(x_{i+1/2-})$ denote left and right reconstructed point values at the cell interface $x_{i+1/2}$. Then the following sign property holds at all interfaces:

$$\begin{cases} \text{if } \bar{v}_{i+1} - \bar{v}_i \geq 0 & \text{then } v_{i+1/2}^+ - v_{i+1/2}^- \geq 0; \\ \text{if } \bar{v}_{i+1} - \bar{v}_i \leq 0 & \text{then } v_{i+1/2}^+ - v_{i+1/2}^- \leq 0. \end{cases} \quad (1.7)$$

In particular, if $\bar{v}_{i+1} = \bar{v}_i$ then the ENO reconstruction is continuous across the interface, $v_{i+1/2}^+ = v_{i+1/2}^-$. Moreover, there is a constant C_p , depending only on p and on the mesh ratio of neighboring grid cells, $\max_{|j-i|\leq p} (|I_{j+1}|/|I_j|)$, such that

$$0 \leq \frac{v_{i+1/2}^+ - v_{i+1/2}^-}{\bar{v}_{i+1} - \bar{v}_i} \leq C_p. \quad (1.8)$$

The sign property tells us that, at each cell interface, the jump of the reconstructed ENO point values cannot have an opposite sign to the jump in the underlying cell averages. The sign property is illustrated in Fig. 1, which shows a third-, fourth- and fifth-order ENO reconstruction of randomly chosen cell averages. Even though the reconstructed polynomial may have large variations within each cell, its jumps at cell interfaces always have the same sign as the jumps of the cell averages. Moreover, the relative size of these jumps is uniformly bounded. We remark that the inequality on the left-hand side of (1.8) is a direct consequence of the sign property (1.7).

Remark 1.1 We emphasize that the main Theorem 1.1 is valid for any order of ENO reconstruction and for any mesh size. It is valid for nonuniform meshes and makes no assumptions on the function v , other than that the cell averages \bar{v}_i must be well defined, which is guaranteed if, e.g., $v \in L^1_{\text{loc}}(\mathbb{R})$. This is a remarkable rigidity property of the piecewise polynomial interpolation.

Remark 1.2 The stability asserted in Theorem 1.1 is realized in terms of the reconstructed point values at cell interfaces $v_{i+1/2}^\pm$. These are precisely the input for the construction of high-order accurate finite volume schemes for nonlinear conservation laws (see Shu [22]), and the relation between these values and the cell averages will be the main point of study in this paper. This approach was taken in [9], where we use the sign property to construct arbitrarily high-order accurate *entropy stable* ENO schemes for systems of conservation laws.

Remark 1.3 The proof of both the sign property and the related upper bound (1.8) depends on the judicious choice of ENO stencils in Algorithm 1.1, and it may fail for

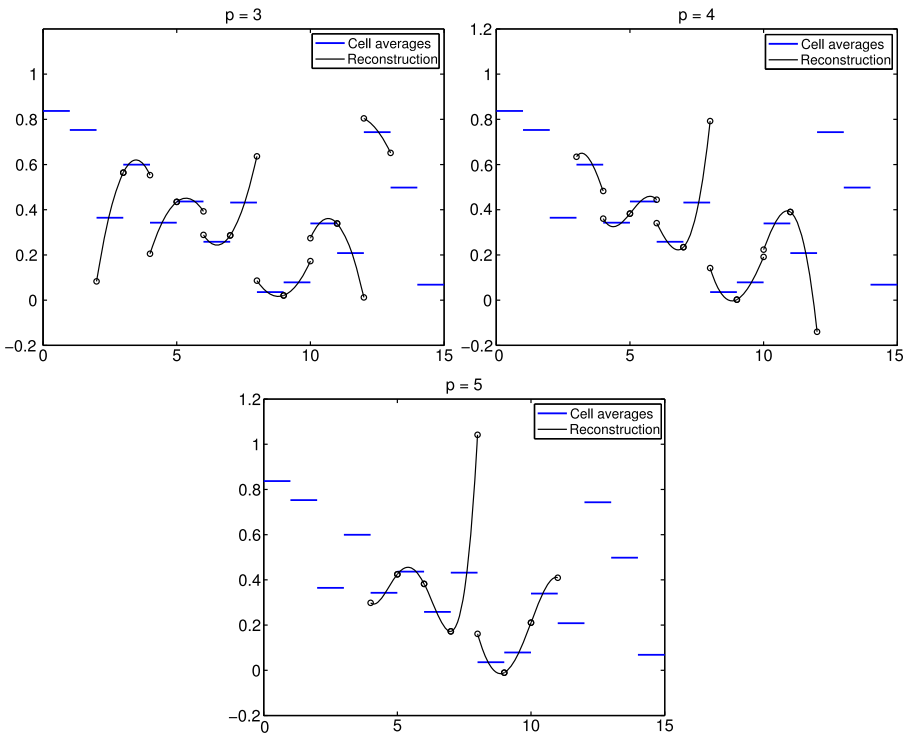


Fig. 1 ENO reconstruction of randomly chosen cell averages

other choices of ENO-based algorithms. In particular, the popular WENO methods, which are based on upwind or central *weighted* ENO stencils [17, 18, 20], fail to satisfy the sign property, as can be easily confirmed numerically.

1.2 ENO Interpolation

The ENO algorithm can be formulated as a nonlinear *interpolation* procedure. The starting point is a given collection of point values, $\{v_i = v(x_i)\}_{i \in \mathbb{Z}}$ at the grid points $\{x_i\}_{i \in \mathbb{Z}}$. The purpose of the ENO procedure in this context (abbreviated \mathcal{I}) is to recover a highly accurate approximation of $v(x)$ from its point values $v_i = v(x_i)$,

$$\text{ENO: } \{v_i\}_i \mapsto \mathcal{I}v(x) := \sum_k f_k(x) \mathbb{1}_{I_k}(x), \quad x_{k \pm 1/2} := \frac{x_k + x_{k+1}}{2}.$$

Here, $f_k(x)$ are polynomials of degree $p - 1$ which interpolate the given data,

$$\mathcal{I}v(x_i) = f_i(x_i) = v_i.$$

Moreover, the ENO interpolant $\mathcal{I}v(x)$ is essentially non-oscillatory in the sense of recovering $v(x)$ to order $\mathcal{O}(h^p)$. In particular, since $v(x)$ may experience jump discontinuities, we wish to recover the point values, $v_{i+1/2}^- := f_i(x_{i+1/2})$ and $v_{i+1/2}^+ :=$

$f_{i+1}(x_{i+1/2})$, with high-order accuracy,

$$|v_{i+1/2}^- - v(x_{i+1/2-})| + |v_{i+1/2}^+ - v(x_{i+1/2+})| = \mathcal{O}(h^p).$$

This version of the ENO procedure was used for finite difference approximation of nonlinear conservation laws in [23]. The ENO interpolant $\mathcal{I}v(x)$ is based on the usual divided differences $\{v[x_i, \dots, x_{i+j}]\}_i$, starting with the grid values $v[x_i] = v_i$ and defined recursively for $j > 0$. Observe that this is less restrictive than the ENO reconstruction, which starts with a pair of neighboring point values $V_{i-1/2}$ and $V_{i+1/2}$.

Let $\{\ell_j\}_{j=1}^p$ be the offsets of the ENO stencil associated with grid point x_i . In this case of ENO interpolation, these offsets are nonpositive integers, corresponding to the integer indices of the prescribed grid points x_j . These offsets are selected according to the following ENO selection procedure.

Algorithm 1.2 (ENO Interpolation: Selection of ENO Stencil) Let point values $v_{i-p+1}, \dots, v_{i+p-1}$ be given:

- Set $\ell_1 = 0$.
- For each $j = 1, \dots, p - 1$, do:

$$\left\{ \begin{array}{l} \text{if } |v[x_{i+\ell_{j-1}}, \dots, x_{i+\ell_j+j-1}]| < |v[x_{i+\ell_j}, \dots, x_{i+\ell_j+j}]| \\ \quad \mapsto \text{ set } \ell_{j+1} = \ell_j - 1, \\ \text{otherwise } \mapsto \text{ set } \ell_{j+1} = \ell_j. \end{array} \right.$$

- Set $f_i(x)$ as the interpolant of v over the stencil $\{v_{i+k}\}_{k=\ell_p}^{\ell_p+p-1}$:

$$f_i(x) = \sum_{j=0}^{p-1} v[x_{i+\ell_j}, \dots, x_{i+\ell_j+j}] \prod_{m=0}^{j-1} (x - x_{i+\ell_j+m}).$$

In the following theorem we state the main stability result for this version of the ENO interpolation procedure, analogous to the sign property of the ENO reconstruction procedure from cell averages.

Theorem 1.2 (The Sign Property Revisited—ENO Interpolation) Fix an integer $p > 1$. Given the point values $\{v_i\}$, let $\mathcal{I}v(x)$ be the p th order ENO interpolant of these point values, outlined in Algorithm 1.2,

$$\mathcal{I}v(x) = \sum_k f_k(x) \mathbb{1}_{I_k}(x), \quad \deg f_k(x) \leq p - 1.$$

Let $v_{i+1/2}^- := \mathcal{I}v(x_{i+1/2-})$ and $v_{i+1/2}^+ := \mathcal{I}v(x_{i+1/2+})$ denote left and right reconstructed point values at the cell interfaces $x_{i+1/2}$. Then the following sign property holds at all interfaces:

$$\left\{ \begin{array}{l} \text{if } v_{i+1} - v_i \geq 0 \quad \text{then } v_{i+1/2}^+ - v_{i+1/2}^- \geq 0; \\ \text{if } v_{i+1} - v_i \leq 0 \quad \text{then } v_{i+1/2}^+ - v_{i+1/2}^- \leq 0. \end{array} \right. \tag{1.9}$$

In particular, if the point values $v_{i+1} = v_i$, then the ENO interpolation is continuous across their midpoints, $v_{i+1/2}^+ = v_{i+1/2}^-$. Moreover, there is a constant c_p , depending only on p and on the mesh ratio $|x_{j+1} - x_j|/|x_j - x_{j-1}|$ of neighboring grid cells, such that

$$0 \leq \frac{v_{i+1/2}^+ - v_{i+1/2}^-}{v_{i+1} - v_i} \leq c_p. \tag{1.10}$$

The rest of this paper is devoted to proving the stability properties of the ENO procedure. We begin with the ENO reconstruction procedure in Theorem 1.1. In Sect. 2 we prove the sign property (1.7), and in Sect. 3 we prove the upper bound (1.8). Similar stability properties hold for the ENO interpolation procedure, dealing with point values instead of cell averages. In Sect. 4 we prove the sign property for the ENO interpolation stated in the main Theorem 1.2. These results were introduced earlier in [8].

2 The Sign Property for ENO Reconstruction

The aim of this section is to prove the sign property (1.7). To this end we derive a novel expression of the interface jump, $v_{i+1/2}^+ - v_{i+1/2}^-$, as a sum of terms which involve $(p + 1)$ th divided differences of V , and we show that each summand in this expression has the same sign as $\bar{v}_{i+1} - \bar{v}_i$.

We recall that at each cell I_i , the ENO reconstruction is based on a particular stencil of $p + 1$ consecutive grid points, $\{x_{i+r}, \dots, x_{i+r+p}\}$, where $r = r(i)$ is the offset of this stencil.

Notation We will reserve the indices r and s to denote offsets of ENO reconstruction stencils. We recall that these offsets measure the shifts to the left of each stencil and are indexed at negative *half-integers*, $-p + 1/2 \leq r, s \leq -1/2$, to match the indexing of cell interfaces at half-integers.

Since this choice of ENO offset depends on the data through the iterative Algorithm 1.1, we need to trace the hierarchy of ENO stencils which ends with the final offset $r = r(i)$. To simplify the notation, we focus our attention on a typical cell I_0 , with an initial stencil which consists of the edges at $x_{-1/2}$ and $x_{1/2}$. The stencil is identified by its leftmost index, $r_1 = -1/2$. Next, the stencil is extended, either to the left, $\{x_{-3/2}, x_{-1/2}, x_{1/2}\}$ where $r_2 = -3/2$, or to the right, $\{x_{-1/2}, x_{1/2}, x_{3/2}\}$ with $r_2 = -1/2$. In the next stage, there are three possible stencils, which are identified by the leftmost offset: $r_3 = -5/2$ corresponding to $\{x_{-5/2}, \dots, x_{1/2}\}$, $r_3 = -3/2$ corresponding to $\{x_{-3/2}, \dots, x_{3/2}\}$, or $r_3 = -1/2$ corresponding to $\{x_{-1/2}, \dots, x_{5/2}\}$. Stage j of the ENO Algorithm 1.1 involves the stencil of $j + 1$ consecutive points, $\{x_{r_j}, \dots, x_{r_j+j}\}$. The series of offsets of this hierarchy of stencils, r_1, r_2, \dots, r_p , forms the *signature* of the ENO algorithm. Note that by our construction,

$$r_1 = -1/2 \geq r_2 \geq r_3 \geq \dots \geq r_p \geq -p + 1/2,$$

and whenever needed, we set $r_{-1} = r_0 = -1/2$. The stability properties of ENO will be proved by carefully studying such data-dependent signatures.

The Newton representation of the p th degree interpolant $F_0(x)$, based on point values $V(x_{r_p}), V(x_{r_p+1}), \dots, V(x_{r_p+p})$, is given by

$$F_0(x) = \sum_{j=0}^p V[x_{r_j}, \dots, x_{r_j+j}] \prod_{m=0}^{j-1} (x - x_{r_j+m}), \tag{2.1}$$

where $V[x_k, \dots, x_{k+j}]$ is the j th divided difference of V at the specified grid points. Observe that in (2.1), we took the liberty of summing the contributions of stencils in their “order of appearance” rather than the usual sum of stencils from left to right.

Notation For notational convenience, we denote the j th divided difference of the primitive V as

$$D_{[r,r+j]} := V[x_r, \dots, x_{r+j}],$$

$$D_{[r,r+j]} = \frac{D_{[r+1,r+j]} - D_{[r,r+j-1]}}{x_{r+j} - x_r}, \quad r = \dots, -3/2, -1/2, 1/2.$$

Thus, for example, by (1.5) we have $D_{[-1/2,3/2]} = V[x_{-1/2}, x_{1/2}, x_{3/2}] = (\bar{v}_1 - \bar{v}_0)/(x_{3/2} - x_{-1/2})$.

If $D_{[-1/2,3/2]} = 0$, or in other words, if $\bar{v}_0 = \bar{v}_1$, then it is easy to see that the ENO procedure will obtain identical stencils for I_0 and I_1 , which in turn yields $v_{1/2}^- = v_{1/2}^+$. We may therefore assume that $D_{[-1/2,3/2]} \neq 0$, and the sign property will be proved by showing that

$$\text{Sign property: } \begin{cases} \text{if } D_{[-1/2,3/2]} > 0 & \text{then } v_{1/2}^+ - v_{1/2}^- \geq 0; \\ \text{if } D_{[-1/2,3/2]} < 0 & \text{then } v_{1/2}^+ - v_{1/2}^- \leq 0. \end{cases} \tag{2.2}$$

To verify (2.2), we examine the ENO reconstruction at cell I_0 , given by $f_0(x) := F'_0(x)$. Differentiation of (2.1) yields

$$f_0(x) = \sum_{j=1}^p D_{[r_j,r_j+j]} \sum_{l=0}^{j-1} \prod_{\substack{m=0 \\ m \neq l}}^{j-1} (x - x_{r_j+m}).$$

The value of f_0 at the cell interface $x_{1/2}$ is then

$$v_{1/2}^- = f_0(x_{1/2}) = \sum_{j=1}^p D_{[r_j,r_j+j]} \sum_{l=0}^{j-1} \prod_{\substack{m=0 \\ m \neq l}}^{j-1} (x_{1/2} - x_{r_j+m})$$

$$= \sum_{j=1}^p D_{[r_j,r_j+j]} \prod_{\substack{m=0 \\ m \neq -r_j+1/2}}^{j-1} (x_{1/2} - x_{r_j+m}). \tag{2.3}$$

The last equality follows from the fact that all but the one term corresponding to $l = -r_j + 1/2$ drop out.

Notation To simplify the notation, we use \prod to denote a product which skips any of its zero factors, $\prod_{j \in J} \alpha_j := \prod_{j \in J: \alpha_j \neq 0} \alpha_j$.

For example, a simple shift of indices in (2.3) yields $v_{1/2}^- = \sum_{j=1}^p D_{[r_j, r_j+j]} \times \prod_{m=-1}^{j-2} (x_{1/2} - x_{r_j+m+1})$. In a similar fashion, we handle the ENO reconstruction at cell I_1 . Let s_1, \dots, s_p be the signature of that cell. Note that $r_j \leq s_j + 1$, since the ENO reconstruction at stage j in cell I_1 cannot select a stencil further to the left than the one used in cell I_0 . If $r_j = s_j + 1$, then the two interpolation stencils are the same, and so $v_{1/2}^+ - v_{1/2}^- = 0$. Hence, we only need to consider the case $r_j \leq s_j$ for all j . The reconstructed value of $f_1(x) = F_1'(x)$ at $x = x_{1/2}$ is given by

$$v_{1/2}^+ = f_1(x_{1/2}) = \sum_{j=1}^p D_{[1+s_j, 1+s_j+j]} \prod_{m=0}^{j-1} (x_{1/2} - x_{s_j+m+1}).$$

The jump in the values reconstructed at $x = x_{1/2}$ is then given by

$$v_{1/2}^+ - v_{1/2}^- = \sum_{j=1}^p \left(D_{[1+s_j, 1+s_j+j]} \prod_{m=0}^{j-1} (x_{1/2} - x_{s_j+m+1}) - D_{[r_j, r_j+j]} \times \prod_{m=-1}^{j-2} (x_{1/2} - x_{r_j+m+1}) \right). \tag{2.4}$$

The following lemma provides a much needed simplification for the rather intimidating expression (2.4), in terms of a key identity, which is interesting in its own right.

Lemma 2.1 *The jump of the reconstructed point values in (2.4) is given by*

$$v_{1/2}^+ - v_{1/2}^- = \sum_{r=r_p}^{s_p} D_{[r, r+p+1]} (x_{r+p+1} - x_r) \prod_{m=0}^{p-1} (x_{1/2} - x_{r+m+1}). \tag{2.5}$$

We postpone the proof of Lemma 2.1 to the end of this section, and we use it in order to conclude the proof of the sign property. To this end, we show that each nonzero summand in (2.5) has the same sign as $\bar{v}_1 - \bar{v}_0$. Since

$$\begin{aligned} \operatorname{sgn} \left((x_{r+p+1} - x_r) \prod_{m=0}^{p-1} (x_{1/2} - x_{r+m+1}) \right) &= (-1)^{r+p-1/2}, \\ r &= -p + 1/2, \dots, -1/2, \end{aligned} \tag{2.6}$$

then in view of (2.2), it remains to prove the following essential lemma.

Lemma 2.2 Let $\{r_j\}_{j=1}^p$ and $\{s_j\}_{j=1}^p$ be the signatures of the ENO stencils associated with cells I_0 and, respectively, I_1 . Then the following holds:

$$\text{if } D_{[-1/2,3/2]} > 0 \text{ then } (-1)^{r+p-1/2} D_{[r,r+p+1]} \geq 0, \quad r = r_p, \dots, s_p, \quad (2.7a)$$

$$\text{if } D_{[-1/2,3/2]} < 0 \text{ then } (-1)^{r+p-1/2} D_{[r,r+p+1]} \leq 0, \quad r = r_p, \dots, s_p. \quad (2.7b)$$

Since r runs over half-integers, (2.7a) and (2.7b) imply that each nonzero term in the sum (2.5) has the same sign as $D_{[-1/2,3/2]}$, and Theorem 1.1 follows from the sign property, (2.2).

Proof We consider the case (2.7a) where $D_{[-1/2,3/2]} > 0$; the case (2.7b) can be argued similarly. The result clearly holds for $p = 1$, where $r_p = s_p = -1/2$ (to clarify matters, we also detail the case $p = 2$ at the end of this section). The general case follows by induction on p . Assuming that (2.7a) and (2.7b) holds for some $p \geq 1$, namely, that $(-1)^{r+p-1/2} D_{[r,r+p+1]} \geq 0$ for $r = r_p, \dots, s_p$, we will verify that it holds for $p + 1$. Indeed,

$$\begin{aligned} & (-1)^{r+p+1/2} D_{[r,r+p+2]} \\ & \equiv (-1)^{r+p+1/2} \frac{D_{[r+1,r+1+p+1]} - D_{[r,r+p+1]}}{x_{r+p+2} - x_r} \\ & = \frac{(-1)^{r+p+1/2} D_{[r+1,r+p+2]} + (-1)^{r+p-1/2} D_{[r,r+p+1]}}{x_{r+p+2} - x_r} \geq 0 \end{aligned} \quad (2.8)$$

for $r = r_p, \dots, s_p - 1$, by the induction hypothesis. Thus, it remains to examine $D_{[r,r+p+2]}$ when $r = r_{p+1} < r_p$ and $r = s_{p+1} \geq s_p$:

- (a) The case $r_{p+1} = r_p$ is already included in (2.8), so the only other possibility is when $r_{p+1} = r_p - 1$. According to the ENO selection principle, this choice of extending the stencil to the left occurs when $|D_{[r_p-1,r_p+p]}| < |D_{[r_p,r_p+p+1]}|$. Consequently, since $(-1)^{r_{p+1}+p+1/2} = (-1)^{r_p+p-1/2}$, and by assumption $(-1)^{r_p+p-1/2} D_{[r_p,r_p+p+1]} = |D_{[r_p,r_p+p+1]}|$, we have

$$\begin{aligned} & (-1)^{r_{p+1}+p+1/2} D_{[r_{p+1},r_{p+1}+p+2]} \\ & \geq \frac{(-1)^{r_p+p-1/2} D_{[r_p,r_p+p+1]} - |D_{[r_p-1,r_p+p]}|}{x_{r_p+p+1} - x_{r_p-1}} > 0, \end{aligned}$$

and (2.7a) follows.

- (b) The case $s_{p+1} = s_p - 1$ is already covered in (2.8). The only other possibility is therefore $s_{p+1} = s_p$. By the ENO selection procedure, this extension to the right occurs when $|D_{[s_{p+1},s_{p+1}+p+2]}| \leq |D_{[s_p,s_p+p+1]}|$. But $(-1)^{s_{p+1}+p+1/2} = -(-1)^{s_p+p-1/2}$ and, by assumption, $(-1)^{s_p+p-1/2} D_{[s_p,s_p+p+1]} = |D_{[s_p,s_p+p+1]}|$,

hence

$$\begin{aligned}
 & (-1)^{s_{p+1}+p+1/2} D_{[s_{p+1}, s_{p+1}+p+2]} \\
 & \geq \frac{-|D_{[s_p+1, s_p+p+2]}| + (-1)^{s_p+p-1/2} D_{[s_p, s_p+p+1]}}{x_{s_p+p+2} - x_{s_p}} \geq 0,
 \end{aligned}$$

and (2.7a) follows. □

Remark 2.1 To further clarify Lemma 2.2, we elaborate here on its proof in the particular case $p = 2$. We assume that $D_{[-1/2, 3/2]} > 0$ and will prove that (2.7a) holds; the other half of Lemma 2.2 in (2.7b) can be proved in a similar manner. The selected stencil for I_0 can be extended in one of two ways. One way is that the ENO stencil associated with I_0 , which starts with $[-1/2, 1/2]$, is extended to the *left*, $[-3/2, 1/2]$, with offset $r_2 = -3/2$; this stencil is selected in the case

$$|D_{[-3/2, 1/2]}| := |\bar{v}_0 - \bar{v}_{-1}| < |\bar{v}_1 - \bar{v}_0| =: |D_{[-1/2, 3/2]}|. \tag{2.9a}$$

The sign property claimed in (2.7a) in this case of an extension to the left with $p = 2$ amounts to

$$(-1)^{r+p-1/2} D_{[r, r+p+1]} = (-1)^{r+3/2} D_{[r, r+3]} \geq 0, \quad r = -3/2, \dots, s_2; \tag{2.9b}$$

here $s = s_2$ is the shift to the left of the stencil associated with cell I_1 . We verify this claim below. The other way is when the ENO stencil associated with I_0 is extended to the *right*, $[-1/2, 3/2]$, with offset $r_2 = -1/2$: this stencil is selected in the case $|\bar{v}_1 - \bar{v}_0| < |\bar{v}_0 - \bar{v}_{-1}|$, and the proof in this case can be argued along the same lines of the left extension outlined below.

Since the left edge of a stencil can be shifted at most one cell to the left, there are only two possibilities of a left shift for the stencil associated with I_1 :

Case (i): $s = -3/2$, that is, the stencil associated with I_1 was extended to the *left* because $|\bar{v}_1 - \bar{v}_0| < |\bar{v}_2 - \bar{v}_1|$. Thus, case (i) holds if $D_{[1/2, 5/2]} > 0$;

Case (ii): $s = -1/2$, that is, the stencil associated with I_1 was extended to the *right* and its left “edge” did not move from its original position at $x = 1/2$, because $|\bar{v}_1 - \bar{v}_0| \geq |\bar{v}_2 - \bar{v}_1|$, namely

$$D_{[-1/2, 5/2]} \leq 0. \tag{2.9c}$$

We now turn to verify (2.9b). In case (i) we have $r = s = -3/2$,

$$(-1)^{r+3/2} D_{[r, r+3]} = D_{[-3/2, 3/2]} := \frac{D_{[-1/2, 3/2]} - D_{[-3/2, 1/2]}}{x_{3/2} - x_{-3/2}}.$$

The expression on the right is indeed nonnegative because $D_{[-1/2, 3/2]} > 0$ by the assumption made in (2.7a), and it dominates $D_{[-3/2, 1/2]}$ by (2.9a).

Next we verify (2.9b) in case (ii) where $s = -1/2$:

$$(-1)^{r+3/2} D_{[r, r+3]} \geq 0, \quad r = -3/2, -1/2. \tag{2.9d}$$

Here there are two subcases, depending on the left shift r :

Case (iia): when $r = -3/2$, we need to verify the positivity claimed in (2.9d), namely,

$$D_{[-3/2,3/2]} := \frac{D_{[-1/2,3/2]} - D_{[-3/2,1/2]}}{x_{3/2} - x_{-3/2}} \geq 0;$$

indeed, this follows by the same arguments as before (note that they are *independent* of the sign of $D_{[1/2,5/2]}$). Thus, the only remaining subcase is

Case (iib): verify (2.9d) with $r = -1/2$ (and recall $s = -1/2$), namely, that $(-1)D_{[-1/2,5/2]} \geq 0$, which clearly holds, since $D_{[-1/2,5/2]}$ in (2.9c) is nonpositive. This concludes the proof of Lemma 2.2 for the case $p = 2$.

We close this section with the promised *proof of Lemma 2.1*.

Proof We proceed in two steps. In the first step, we consider the special case when the two stencils that are used by the ENO reconstruction in cells I_0 and I_1 are only one grid cell apart. Such stencils must have the same offset, say $r_p = s_p = r$, and in this case, Lemma 2.1 claims that $v_{1/2}^+ - v_{1/2}^-$ equals

$$f_1(x_{1/2}) - f_0(x_{1/2}) = D_{[r,r+p+1]}(x_{r+p+1} - x_r) \prod_{m=0}^{p-1} (x_{1/2} - x_{r+m+1}). \tag{2.10}$$

Indeed, the interpolant of $V(x_{r+1}), \dots, V(x_{r+p}), V(x_r)$, assembled in the specified order from left to right and then adding $V(x_r)$ at the end, is given by

$$F_0(x) = \sum_{j=0}^{p-1} D_{[r+1,r+1+j]} \prod_{m=0}^{j-1} (x - x_{r+1+m}) + D_{[r,r+p]} \prod_{m=0}^{p-1} (x - x_{r+1+m}).$$

Similarly, the interpolant of $V(x_{r+1}), \dots, V(x_{r+p+1})$, assembled in the specified order from left to right, is given by

$$F_1(x) = \sum_{j=0}^{p-1} D_{[r+1,r+j+1]} \prod_{m=0}^{j-1} (x - x_{r+1+m}) + D_{[r+1,r+p+1]} \prod_{m=0}^{p-1} (x - x_{r+1+m})$$

(cf. (2.1)). Thus, their difference amounts to

$$\begin{aligned} F_1(x) - F_0(x) &= (D_{[r+1,r+p+1]} - D_{[r,r+p]}) \prod_{m=0}^{p-1} (x - x_{r+1+m}) \\ &= D_{[r,r+p+1]}(x_{r+p+1} - x_r) \prod_{m=0}^{p-1} (x - x_{r+1+m}), \end{aligned}$$

which reflects the fact that F_0 and F_1 coincide at the p points x_{r+1}, \dots, x_{r+p} . Differentiation yields

$$f_1(x) - f_0(x) = D_{[r,r+p+1]}(x_{r+p+1} - x_r) \sum_{l=0}^{p-1} \prod_{\substack{m=0 \\ m \neq l}}^{p-1} (x - x_{r+1+m}).$$

At $x = x_{1/2}$, all product terms on the right vanish except for $l = -r - 1/2$, since $x_{1/2}$ belongs to both stencils. We obtain

$$f_1(x_{1/2}) - f_0(x_{1/2}) = D_{[r,r+p+1]}(x_{r+p+1} - x_r) \prod_{m=0}^{p-1} (x_{1/2} - x_{r+m+1}).$$

This shows that (2.10) holds, verifying Lemma 2.1 in the case that the stencils associated with I_0 and I_1 are separated by just one cell.

In step two, we extend this result for arbitrary stencils, where I_0 and I_1 are associated with arbitrary offsets, $r_p \leq s_p$. Denote by $F^{(j)}$ the interpolant at points x_j, \dots, x_{j+p} , so that $F_0 = F^{(r_p)}$ and $F_1 = F^{(s_p+1)}$. Using the representation from the first step for the difference of one-cell shifted stencils, $(f^{(r+1)} - f^{(r)})(x_{1/2})$, we can write the jump at the cell interface as a telescoping sum,

$$\begin{aligned} (f_1 - f_0)(x_{1/2}) &= (f^{(s_p+1)} - f^{(r_p)})(x_{1/2}) \\ &= \sum_{r=r_p}^{s_p} (f^{(r+1)} - f^{(r)})(x_{1/2}) \\ &= \sum_{r=r_p}^{s_p} D_{[r,r+p+1]}(x_{r+p+1} - x_r) \prod_{m=0}^{p-1} (x_{1/2} - x_{r+m+1}), \end{aligned}$$

and (2.5) follows. □

3 The Relative Jumps in ENO Reconstruction Are Bounded

In this section, we will prove (1.8), which establishes an upper bound on the size of the jump in reconstructed values in terms of the jump in the underlying cell averages. We need the following lemma.

Lemma 3.1 *Let r_p, s_p be the (half-integer) offsets of the ENO stencils associated with cell I_0 and, respectively, I_1 . Then*

$$\frac{D_{[r,r+p+1]}}{D_{[-1/2,3/2]}} (-1)^{r+p-1/2} \leq C_{r,p}, \quad r = r_p, \dots, s_p, \tag{3.1a}$$

where the constants $C_{r,p}$ are defined recursively, starting with $C_{r,1} = 1$, and

$$C_{r,p+1} = \frac{2}{x_{r+p+2} - x_r} \max(C_{r,p}, C_{r+1,p}) \quad \forall r. \tag{3.1b}$$

The quantity on the left in (3.1a) was shown to be bounded from below by zero in Lemma 2.2; here we prove an upper bound. The constants $C_{r,p}$ only depend on the grid sizes $|I_j|$.

Proof The result clearly holds for $p = 1$. We prove the general induction step passing from $p \mapsto p + 1$. Using the recursion relation

$$D_{[r,r+p+2]} = \frac{D_{[r+1,r+p+2]} - D_{[r,r+p+1]}}{\Delta x}, \quad \Delta x := x_{r+p+2} - x_r,$$

we have

$$\begin{aligned} 0 &\leq \frac{D_{[r,r+p+2]}}{D_{[-1/2,3/2]}} (-1)^{r+p+1/2} \\ &= \frac{1}{\Delta x} \left(\frac{D_{[r+1,(r+1)+p+1]}}{D_{[-1/2,3/2]}} (-1)^{r+p+1/2} + \frac{D_{[r,r+p+1]}}{D_{[-1/2,3/2]}} (-1)^{r+p-1/2} \right) \\ &\leq \frac{C_{r+1,p} + C_{r,p}}{\Delta x} \leq C_{r,p+1}, \quad r = r_p, \dots, s_p - 1. \end{aligned} \tag{3.2}$$

We turn to the remaining cases:

- (a) As in Lemma 2.2, if $r_{p+1} = r_p$ then the induction step is already covered in (3.2), so the only remaining case is $r = r_{p+1} = r_p - 1$, corresponding to Lemma 2.2(a). In this case, $|D_{[r,r+p+2]}| \leq |D_{[r+1,r+p+2]}|$, hence

$$\begin{aligned} \frac{D_{[r,r+p+2]}}{D_{[-1/2,3/2]}} (-1)^{r+p+1/2} &= \frac{1}{\Delta x} \frac{D_{[r+1,r+p+2]} - D_{[r,r+p+1]}}{D_{[-1/2,3/2]}} (-1)^{r+p+1/2} \\ &\leq \frac{2}{\Delta x} \frac{D_{[r+1,r+p+2]}}{D_{[-1/2,3/2]}} (-1)^{r+p+1/2} \\ &\leq \frac{2C_{r+1,p}}{\Delta x} \leq C_{r,p+1}. \end{aligned}$$

- (b) If $s_{p+1} = s_p - 1$ then the induction step is already covered in (3.2), so the only remaining case is $r = s_{p+1} = s_p$, corresponding to Lemma 2.2(b). In this case, $|D_{[r+1,r+p+2]}| \leq |D_{[r,r+p+1]}|$, hence

$$\begin{aligned} \frac{D_{[r,r+p+2]}}{D_{[-1/2,3/2]}} (-1)^{r+p+1/2} &= \frac{1}{\Delta x} \frac{D_{[r+1,r+p+2]} - D_{[r,r+p+1]}}{D_{[-1/2,3/2]}} (-1)^{r+p+1/2} \\ &\leq \frac{2}{\Delta x} \frac{D_{[r,r+p+1]}}{D_{[-1/2,3/2]}} (-1)^{r+p-1/2} \leq \frac{2C_{r,p}}{\Delta x} \leq C_{r,p+1}. \end{aligned}$$

□

Using the explicit form (2.5) of the jump $v_{1/2}^+ - v_{1/2}^-$, we get the following explicit expression of the upper bound asserted in (1.8).

Theorem 3.2 Let $v_{1/2}^+$ and $v_{1/2}^-$ be the point values reconstructed by the ENO algorithm 1.1 at the cell interface $x = x_{1/2}^+$ and, respectively, $x = x_{1/2}^-$. Then

$$\frac{v_{1/2}^+ - v_{1/2}^-}{\bar{v}_1 - \bar{v}_0} \leq C_p := \frac{1}{x_{3/2} - x_{-1/2}} \times \sum_{r=-p+1/2}^{-1/2} C_{r,p} \left| (x_{r+p+1} - x_r) \prod_{m=0}^{p-1} (x_{1/2} - x_{r+m+1}) \right|.$$

Proof Let r_p, s_p be the offsets of the ENO stencils associated with cell I_0 and, respectively, I_1 . By Lemmas 2.1 and 3.1, we have

$$\begin{aligned} \frac{v_{1/2}^+ - v_{1/2}^-}{\bar{v}_1 - \bar{v}_0} &= \frac{1}{x_{3/2} - x_{-1/2}} \times \sum_{r=r_p}^{s_p} \frac{D_{[r,r+p+1]}}{D_{[-1/2,3/2]}} (-1)^{r+p-1/2} \left| (x_{r+p+1} - x_r) \prod_{m=0}^{p-1} (x_{1/2} - x_{r+m+1}) \right| \\ &\leq \frac{1}{x_{3/2} - x_{-1/2}} \sum_{r=r_p}^{s_p} C_{r,p} \left| (x_{r+p+1} - x_r) \prod_{m=0}^{p-1} (x_{1/2} - x_{r+m+1}) \right| \\ &\leq \frac{1}{x_{3/2} - x_{-1/2}} \sum_{r=-p+1/2}^{-1/2} C_{r,p} \left| (x_{r+p+1} - x_r) \prod_{m=0}^{p-1} (x_{1/2} - x_{r+m+1}) \right|. \end{aligned}$$

□

When the mesh is uniform, $|I_i| \equiv h$, the expression for the upper bound C can be calculated explicitly. The recursion relation (3.1b) yields $C_{r,p} = \frac{2^p}{h^{p-1}(p+1)!}$, and the coefficient of the $(p + 1)$ th order divided differences in (2.5) is

$$\left| (x_{r+p+1} - x_r) \prod_{m=0}^{p-1} (x_{1/2} - x_{r+m+1}) \right| = h^p (p + 1)(-r - 1/2)!(p + r - 1/2)!.$$

Thus, we arrive at the following bound on the jump in reconstructed values.

Corollary 3.3 Let $v_{1/2}^+$ and $v_{1/2}^-$ be the point values reconstructed at the cell interface $x = x_{1/2}^+$ and, respectively, $x = x_{1/2}^-$, by the p th order ENO Algorithm 1.1, based on equispaced cell averages $\{\bar{v}_k\}_k$. Then

$$\frac{v_{1/2}^+ - v_{1/2}^-}{\bar{v}_1 - \bar{v}_0} \leq C_p = 2^{p-1} \frac{1}{p!} \sum_{k=0}^{p-1} k!(p - k - 1)! \tag{3.3}$$

Table 1 shows the upper bound (3.3) on $(v_{1/2}^+ - v_{1/2}^-)/(\bar{v}_1 - \bar{v}_0)$ for some values of p . Returning to Fig. 1, we see that, although the jumps at the cell interfaces can

Table 1 Maximal ratio of jumps in ENO reconstruction of order p , relative to underlying jumps of averages at cell interfaces

p	Upper bound C_p
1	1
2	2
3	$10/3 = 3.333\dots$
4	$16/3 = 5.333\dots$
5	$128/15 = 8.533\dots$
6	$208/15 = 13.866\dots$

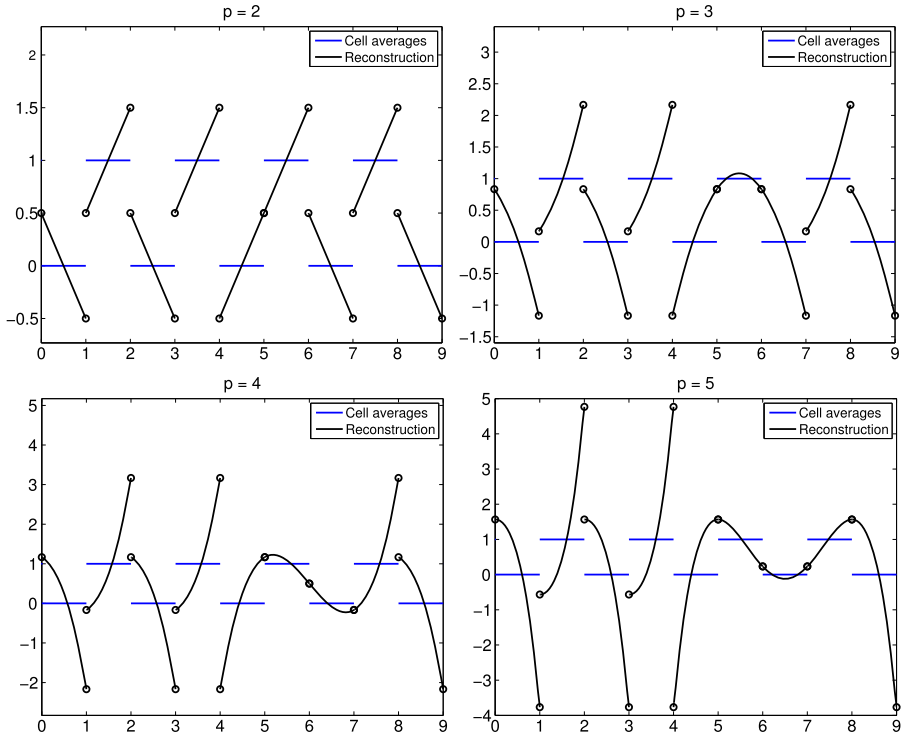


Fig. 2 Worst-case cell interface jumps for $p = 2, 3, 4, 5$

become large, they *cannot* exceed C_p times the size of the jump in cell averages, regardless of the values in neighboring cell averages.

It can be shown that the bound C_p given in Theorem 3.2 is sharp. Indeed, the worst-case scenarios for orders of accuracy $p = 2, 3, 4, 5$ are shown in Fig. 2. The mesh in this figure is $x_{i+1/2} = i$, and the cell averages are chosen as

$$\bar{v}_i = \begin{cases} 0 & \text{if } i \text{ is odd,} \\ 1 & \text{if } i \text{ is even and } i \leq 4, \\ 1 - 10^{-10} & \text{if } i \text{ is even and } i > 4. \end{cases}$$

The number 10^{-10} is chosen at random; any small perturbation will give the same effect. This perturbation ensures that cells I_i for $i \leq 4$ interpolate over a stencil to the left of the cell interface $x = x_{4+1/2}$, and cells with $i > 4$ to the right of it. We see that for each p , the jump at $x = 4$ is precisely the bound C_p as given in Table 1.

4 ENO Interpolation

The stability proof of ENO interpolation stated in Theorem 1.2 can be argued along the lines of those argued in Sects. 2 and 3. We therefore only sketch the arguments without details.

4.1 The Sign Property for ENO Interpolant

We focus on the jump across the interface at $x = x_{1/2}$. Let $\{\ell_j\}_{j=1}^p$ and $\{n_j\}_{j=1}^p$ be the ENO stencils associated, respectively, with grid points x_0 and x_1 . Recall that in this case of ENO interpolation, these offsets are nonpositive integers, $-p + 1 \leq \ell_j, n_j \leq 0$. Our first key step is to compute the jump at the interface point $x_{1/2}$ in the case where the ENO procedures are separated by just one point, namely, $\ell_p = n_p$. We let $d_{[i,i+j]}$ abbreviate the divided differences $v[x_i, \dots, x_{i+j}]$. As before, we denote the reconstructed values at the interface $x = x_{1/2}$ by $v_{1/2}^- = \mathcal{I}v(x_{1/2}-)$ and $v_{1/2}^+ = \mathcal{I}v(x_{1/2}+)$.

Lemma 4.1 *If $\ell_p = n_p = \ell$ for some $\ell \in -\mathbb{N}_0$, then*

$$v_{1/2}^+ - v_{1/2}^- = d_{[\ell, \ell+p+1]}(x_{\ell+p+1} - x_\ell) \prod_{m=1}^{p-1} (x_{1/2} - x_{\ell+m}).$$

By assembling a telescoping sum of several such stencils, we obtain

Corollary 4.2 *For general $\ell_p \leq n_p$, we have*

$$v_{i+1/2}^+ - v_{i+1/2}^- = \sum_{\ell=\ell_p}^{n_p} d_{[\ell, \ell+p+1]}(x_{\ell+p+1} - x_\ell) \prod_{m=1}^{p-1} (x_{1/2} - x_{\ell+m}). \tag{4.1}$$

Since $v_1 - v_0 = (x_1 - x_0)d_{[0,1]}$, we wish to show that the jump in reconstructed values at the cell interface has the same sign as $d_{[0,1]}$. To this end we show that each summand in (4.1) has the same sign as $d_{[0,1]}$. Indeed, since

$$\text{sgn} \left((x_{\ell+p} - x_\ell) \prod_{m=1}^{p-1} (x_{1/2} - x_{\ell+m}) \right) = (-1)^{\ell+p+1}, \quad -p + 1 \leq \ell \leq 0,$$

it suffices to prove the following.

Lemma 4.3 *If ℓ_p, n_p are selected according to the ENO stencil selection procedure, then*

$$\begin{cases} \text{if } d_{[0,1]} \geq 0 & \text{then } (-1)^{\ell+p+1} d_{[\ell, \ell+p+1]} \geq 0; \\ \text{if } d_{[0,1]} \leq 0 & \text{then } (-1)^{\ell+p+1} d_{[\ell, \ell+p+1]} \leq 0, \end{cases} \quad \ell = \ell_p, \dots, n_p.$$

4.2 Upper Bounds on the Relative Jumps for ENO Interpolant

Next, we show the corresponding upper bound on $v_{1/2}^+ - v_{1/2}^-$ for ENO reconstruction with point values.

Lemma 4.4 *If ℓ_p, n_p are selected according to the ENO stencil selection procedure, then*

$$0 \leq \frac{d_{[\ell, \ell+p+1]}}{d_{[0,1]}} (-1)^{\ell+p+1} \leq c_{\ell,p} \quad \ell = \ell_p, \dots, n_p,$$

where $c_{\ell,p}$ are defined recursively, starting with $c_{\ell,1} = 1$, and

$$c_{\ell,p+1} = \frac{2}{x_{\ell+p} - x_\ell} \max(c_{\ell,p}, c_{\ell+1,p}).$$

For simplicity we assume that the mesh is uniform with mesh width $x_{j+1} - x_j \equiv h$. It is straightforward to show that $c_{\ell,p} \equiv (2/h)^{p-1} 1/p!$. Moreover, the coefficient of the $(p + 1)$ th order divided differences in (4.1) is

$$\left| (x_{\ell+p} - x_\ell) \prod_{m=1}^{p-1} (x_{1/2} - x_{\ell+m}) \right| = h^p p \left| \prod_{m=1}^{p-1} (1/2 - \ell - m) \right|.$$

Thus, we arrive at the following bound on the jump in reconstructed values.

Theorem 4.5 *Let ℓ_p, n_p be selected according to the ENO stencil selection procedure, and assume that the mesh is uniform. Then*

$$\frac{v_{1/2}^+ - v_{1/2}^-}{v_1 - v_0} \leq c_p := 2^{p-1} \frac{1}{(p-1)!} \sum_{\ell=0}^{p-1} \left| \prod_{m=1}^{p-1} (1/2 - \ell - m) \right|.$$

Table 2 Maximal ratio of jumps in ENO interpolation of order p , relative to underlying jumps of point values at midpoints

p	Upper bound c_p
1	1
2	2
3	3.5
4	6
5	10.375
6	18.25

Table 2 shows the upper bound on $(v_{1/2}^+ - v_{1/2}^-)/(v_1 - v_0)$ for $p \leq 6$. As for the ENO reconstruction procedure in Sect. 3, it may be shown that these bounds are sharp.

5 Conclusions

We show that the ENO reconstruction procedure (from cell averages or point values) is stable via the *sign property*; that is, the jump in reconstructed values at each cell interface has the same sign as the jump in the underlying cell averages (point values). Furthermore, we obtain an upper bound on the size of the jump of reconstructed values in terms of the underlying cell averages (point values) at each interface. Both results hold for any mesh $\{x_{i+1/2}\}_i$. In particular, the results hold for nonuniform meshes. In addition, both results hold for *any* order of the reconstruction, i.e., any degree for the polynomial interpolation. No extra regularity assumptions on the underlying L^1_{loc} function v are needed.

The proofs of both the sign property and the upper jump bound depended heavily on the formula (2.5), which gives the cell interface jump in terms of r_p , s_p , and the $(p + 1)$ th divided differences of V . This formula is completely independent of the ENO stencil selection procedure, and hence holds for *all* interpolation stencils. However, Lemma 2.2 (and Lemma 3.1 for the upper bound) is a direct consequence of the ENO stencil procedure. Therefore, we cannot expect that other reconstruction methods will satisfy a similar sign property. In particular, the WENO method, using the stencil weights proposed in [17, 20], will generally *not* satisfy such a property, a fact that is easily confirmed numerically. This leaves open the question of the existence of stencil weights that make the method satisfy the sign property. Of the second-order TVD reconstruction methods (see [24]), only the minmod limiter satisfies the sign property.

The stability estimates presented in this paper do not suffice to conclude that the ENO reconstruction procedure is total variation bounded (TVB). In particular, the jump in the interior of a cell can be large. However, the sign property enables us to construct arbitrarily high-order *entropy stable* schemes for any system of conservation laws. Furthermore, the sign property together with the upper bound allow us to prove that these entropy stable schemes converge for linear equations. Both results are introduced in [8] and presented in a forthcoming paper [9].

Acknowledgements S.M. thanks Prof. Mike Floater of CMA, Oslo for useful discussions. The research of E.T. was supported by grants from the National Science Foundation, DMS#10-08397, and the Office of Naval Research, ONR#N000140910385 and #000141210318.

References

1. S. Amat, F. Arandiga, A. Cohen, R. Donat, Tensor product multiresolution with error control, *Signal Process.*, **82**, 587–608 (2002).
2. F. Arandiga, A. Cohen, R. Donat, N. Dyn, Interpolation and approximation of piecewise smooth functions, *SIAM J. Numer. Anal.* **43**(1), 41–57 (2005).

3. F. Arandiga, A. Cohen, R. Donat, N. Dyn, B. Matei, Approximation of piecewise smooth functions and images by edge-adapted (ENO-EA) nonlinear multiresolution techniques, *Appl. Comput. Harmon. Anal.*, **24**, 225–250 (2008).
4. R. Baraniuk, R. Claypoole, G.M. Davis, W. Sweldens, Nonlinear wavelet transforms for image coding via lifting, *IEEE Trans. Image Process.*, **12**, 1449–1459 (2003).
5. M. Berzins, Adaptive polynomial interpolation on evenly spaced meshes, *SIAM Rev.* **49**(4), 604–627 (2007).
6. T. Chan, H.M. Zhou, ENO-wavelet transforms for piecewise smooth functions, *SIAM J. Numer. Anal.*, **40**(4), 1369–1404 (2002).
7. A. Cohen, N. Dyn, M. Matel, Quasilinear subdivision schemes with applications to ENO interpolation, *Appl. Comput. Harmon. Anal.*, **15**, 89–116 (2003).
8. U.S. Fjordholm, S. Mishra, E. Tadmor, Entropy stable ENO scheme, in *Hyperbolic Problem: Theory, Numerics and Applications. Proc. of HYP2010—the 13th International Conference on Hyperbolic Problems Held in Beijing* (2012, to appear).
9. U.S. Fjordholm, S. Mishra, E. Tadmor, Arbitrarily high-order essentially non-oscillatory entropy stable schemes for systems of conservation laws, *SIAM J. Numer. Anal.* (in press).
10. A. Harten, ENO schemes with subcell resolution, *J. Comput. Phys.* **83**, 148–184 (1989).
11. A. Harten, Recent developments in shock-capturing schemes, in *Proc. International Congress of Mathematicians, vols. I, II*, Kyoto, 1990 (Math. Soc. Japan, Tokyo, 1991), pp. 1549–1559.
12. A. Harten, Multi-resolution analysis for ENO schemes, in *Algorithmic Trends in Computational Fluid Dynamics (1991)* (Springer, New York, 1993), pp. 287–302.
13. A. Harten, Adaptive multiresolution schemes for shock computations, *J. Comput. Phys.* **115**(2), 319–338 (1994).
14. A. Harten, Multiresolution representation of cell-averaged data: a promotional review, in *Signal and Image Representation in Combined Spaces*. Wavelet Anal. Appl., vol. 7 (Academic Press, San Diego, 1998), pp. 361–391.
15. A. Harten, B. Engquist, S. Osher, S.R. Chakravarty, Some results on high-order accurate essentially non-oscillatory schemes, *Appl. Numer. Math.* **2**, 347–377 (1986).
16. A. Harten, B. Engquist, S. Osher, S.R. Chakravarty, Uniformly high order accurate essentially non-oscillatory schemes, *J. Comput. Phys.* **71**(2), 231–303 (1987).
17. G. Jiang, C.-W. Shu, Efficient implementation of weighted ENO schemes, *J. Comput. Phys.* **126**, 202–226 (1996).
18. D. Levy, G. Puppo, G. Russo, Central WENO schemes for hyperbolic systems of conservation laws, *Math. Model. Numer. Anal.* **33**, 547–571 (1999).
19. B. Matei, Méthodes multirésolution non-linéaires- applications au traitement d’image. Ph.D. thesis, University Paris VI (2002).
20. J. Qiu, C.-W. Shu, On the construction, comparison, and local characteristic decompositions for high order central WENO schemes, *J. Comput. Phys.* **183**, 187–209 (2002).
21. C.W. Shu, Numerical experiments on the accuracy of ENO and modified ENO schemes, *J. Sci. Comput.* **5**(2), 127–149 (1990).
22. C.W. Shu, Essentially non-oscillatory and weighted essentially non-oscillatory schemes for hyperbolic conservation laws. ICASE Technical report, NASA, 1997.
23. C.W. Shu, S. Osher, Efficient implementation of essentially non-oscillatory schemes—II, *J. Comput. Phys.* **83**, 32–78 (1989).
24. P. Sweby, High resolution schemes using flux limiters for hyperbolic conservation laws, *SIAM J. Numer. Anal.* **21**, 995–1011 (1984).